Energy Efficient Relay for Unmanned Aerial Vehicle with Onboard Hybrid Reconfigurable Intelligent Surfaces

Chi Yen Goh[1], Chee Yen Leow[1], Chuan Heng Foh[2], Igbafe Orikumhi[3], Sunwoo Kim[3], and Jinsong Wu[4]
[1]Wireless Communication Centre, Faculty of Electrical Engineering, Universiti Teknologi Malaysia, Johor, Malaysia.
[2]5GIC&6GIC, Institute for Communication Systems (ICS), University of Surrey, Guildford, U.K.
[3]Department of Electronic Engineering, Hanyang University, Seoul, South Korea.
[4]School of Artificial Intelligence, Guilin University of Electronic Technology, 510004, China, and Department of Electrical Engineering, University of Chile, 8370451, Chile.
Email: {yen1997@graduate, bruceleow@}.utm.my, c.foh@surrey.ac.uk, {oigbafe2@, remero@}hanyang.ac.kr, wujs@ieee.org

***Abstract*—Reconfigurable Intelligent Surfaces (RIS) and Unmanned Aerial Vehicles (UAVs) have emerged as promising technologies for the 6th-Generation (6G) network. The integration of RIS with the UAV (RIS-UAV) can enhance ground communication by providing a 360° panoramic reflection. Existing RIS-UAV mainly considers passive elements which suffer from double path loss problems. This motivates the use of the hybrid RIS-UAV equipped with both active and passive RIS elements. This paper investigates the energy efficiency maximisation problem for the hybrid RIS-UAV by optimising the placement of the UAV, subject to the UAV's permitted altitude range. The non-convex optimisation problem is addressed using Particle Swarm Optimisation (PSO) tool and distributed learning algorithm. The numerical results show that the proposed distributed learning algorithm is preferred when optimising the energy efficiency of the hybrid RIS-UAV system. In addition, hybrid RIS-UAV outperforms the fully passive RIS-UAV and the active amplify-and-forward (AF) relay in terms of energy efficiency of the system.**

***Index Terms*—Reconfigurable intelligent surfaces, unmanned aerial vehicles, energy efficiency, distributed learning, wireless communication**

I. Introduction

Reconfigurable intelligent surfaces (RIS) are reconfigurable metasurfaces that are made up of a two-dimensional array of low-cost reflecting elements that can be controlled to manipulate the radio propagation environment [1]. Recently, the integration of RIS with unmanned aerial vehicles (UAV) has emerged as a promising solution to enhance UAV cooperative communication, where the UAVs serve as aerial RIS to assist the communication system. RIS-UAV is the term that refers to the integration of RIS and UAV throughout this paper. By mounting the RIS on the surface of the UAV, the three-dimensional (3D) flexibility and mobility of UAV can be used to provide a 360° panoramic reflection for the incident signals instead of the 180° half-space reflection provided by the conventional terrestrial RIS that are static [2], [3]. Therefore, the RIS-UAV has been widely studied as an aerial RIS to assist the wireless communication system.

However, the existing RIS-UAV mainly consists of passive elements that only reflect the incident signals without modifying them. Thus, the received signals reflected by the passive RIS-UAV experience double path loss problem [4]. To overcome these issues, a hybrid RIS-UAV consisting of both active and passive elements has been introduced [5]. By adding the active load impedance, the hybrid RIS-UAV can amplify the signal while reflecting it towards the desired destination. This approach results in improved signal quality compared to the passive RIS-UAV. Additionally, when compared to the fully active RIS-UAV that demands a larger power budget, the hybrid RIS-UAV emerges as the optimal choice.

There have been several studies on optimising the passive RIS-UAV and the hybrid terrestrial RIS. In [6], [7], UAV trajectory, transmit beamforming at the base station (BS) and passive beamforming of the passive RIS were jointly optimised to maximise the average achievable rate and the average secrecy rate of the passive RIS-UAV communication system, respectively. To exploit the advantages of passive RIS and the UAV active relay, [8] studied the integrated passive RIS and UAV active relay system by selecting the transmission mode between the passive RIS-UAV and UAV active relay. Besides, the paper optimised the altitude of the UAV, the number of RIS elements and the transmission mode to maximise the system capacity and energy efficiency. By optimising the transmit beamforming at the BS and hybrid terrestrial RIS, [9] demonstrates that the hybrid terrestrial RIS, which utilizes a single active element, achieves an improvement of about 40% in spectral efficiency if compared to the conventional passive terrestrial RIS. Nevertheless, none of the studies consider the optimisation of the hybrid RIS-UAV.

This paper aims to maximise the energy efficiency of the hybrid RIS-UAV by optimising the placement of the UAV, subject to the permitted altitude range of the UAV. Two optimisation approaches are studied, Particle Swarm Optimisation (PSO) and the distributed learning. Besides, the energy efficiency of the optimised hybrid RIS-UAV is analysed and compared

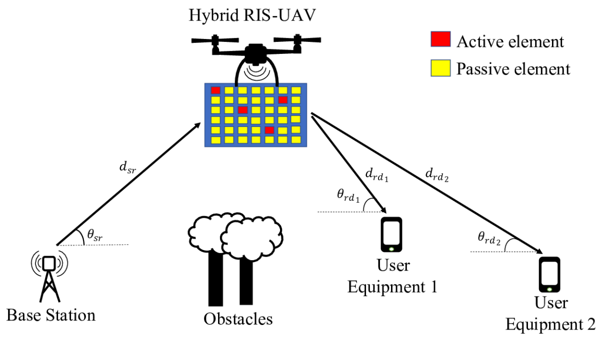

Fig. 1. Hybrid RIS-UAV cooperative communication.

to that of the conventional passive RIS-UAV, as well as the active relay. The numerical results are provided to highlight the potential of the hybrid RIS-UAV for multiple users. In addition, the numerical results show that the optimal UAV position that maximises the energy efficiency of the system can be computed in a shorter time by implementing the proposed distributed learning rather than the PSO algorithm.

The paper is organised as follows. In Section II, the system model of the hybrid RIS-UAV is introduced and the energy efficiency maximisation problem is formulated. In addition, the two algorithms used to solve the optimisation problem are described in that section. Numerical results are presented and discussed in Section III, and conclusions are drawn in Section IV.

II. System Model

As shown in Fig. 1, we consider a downlink communication system assisted by a hybrid RIS-UAV, in which the RIS that is mounted on the rotary-wing UAV, consists of both active and passive reflecting elements. Assuming that the direct link between the BS and the user equipment (UEs) are blocked, hence the hybrid RIS-UAV serves as a mobile aerial RIS to amplify and reflect the signal from the BS towards the UEs within a finite flying time T seconds. The flying time is equally divided into a total time slot N, with a slot width of δ, such that $T = \delta N$. The BS is assumed to be fixed at the origin while the UEs are moving with positive x-axis and y-axis. On the other hand, the hybrid RIS-UAV hovers at a certain altitude, z_{UAV} while forwarding the signals. Since each of the RIS elements is assumed half of the wavelength size, therefore the signals are reflected with a constant gain from the elements.

Assuming that the distance between BS and the k-th RIS elements are approximately same with the distance between BS and the UAV, and the distance between k-th RIS elements and UEs is the same with the distance between UAV and the UEs. The locations of the BS, hybrid RIS-UAV, and the UE in 3D Cartesian coordinates are $\boldsymbol{w}_{BS}[n] = (x_{BS}[n], y_{BS}[n], \mathit{0})$, $\boldsymbol{w}_{UAV}[n] = (x_{UAV}[n], y_{UAV}[n], z_{UAV}[n])$, and $\boldsymbol{w}_{UE_j}[n] = \left(x_{UE_j}[n], y_{UE_j}[n], \mathit{0}\right)$, respectively, with $j = \{1, 2\}$. Hence, the distance between the BS and the hybrid RIS-UAV at n-th time slot can be computed as:

$$d_{sr}[n] = \sqrt{\mid \boldsymbol{w}_{UAV}[n] - \boldsymbol{w}_{BS}[n] \mid^2}, \tag{1}$$

while the distance between the hybrid RIS-UAV and the UEs at n-th time slot is defined as:

$$d_{rd_j}[n] = \sqrt{\mid \boldsymbol{w}_{UAV}[n] - \boldsymbol{w}_{UE}[n] \mid^2}. \tag{2}$$

The channels between the hybrid RIS-UAV and the ground nodes are modeled using Al-Hourani's channel model with Rician small-scale fading [10], [11]. For each channel, the probability of line-of-sight (LoS) is defined as:

$$P_{LoS}(\theta_r[n]) = \frac{1}{1 + a\exp(-b[\theta_r[n] - a])}, \tag{3}$$

where a and b are constant environmental variables, and θ_r represents the elevation angle between the hybrid RIS-UAV and the ground nodes, where $r = \{sr, rd_1, rd_2\}$. Accordingly, the elevation angle between the BS and the hybrid RIS-UAV at n-th time slot is defined as:

$$\theta_{sr}[n] = \tan^{-1}\left(\frac{z_{UAV}[n]}{d_1[n]}\right), \tag{4}$$

$$d_1[n] = \mid x_{UAV}[n] - x_{BS}[n] \mid + \mid y_{UAV}[n] - y_{BS}[n] \mid, \tag{5}$$

while the elevation angle between the hybrid RIS-UAV and the UEs at n-th time slot is defined as:

$$\theta_{rd_j}[n] = \tan^{-1}\left(\frac{z_{UAV}[n]}{d_{2_j}[n]}\right), \tag{6}$$

$$d_{2_j}[n] = \mid x_{UAV}[n] - x_{UE_j}[n] \mid + \mid y_{UAV}[n] - y_{UE_j}[n] \mid. \tag{7}$$

Meanwhile, the channel gains between the BS and the hybrid RIS-UAV, and between the hybrid RIS-UAV and the UEs, are given as [11]:

$$\mid h_{sr}[n] \mid^2 = \frac{A \mid \Omega_{sr}[n] \mid^2}{d_{sr}[n]^{\alpha_{sr}[n]}}, \tag{8}$$

$$\mid h_{rd_j}[n] \mid^2 = \frac{A \mid \Omega_{rd_j}[n] \mid^2}{d_{rd_j}[n]^{\alpha_{rd_j}[n]}}, \tag{9}$$

respectively. The parameter A is a constant that represents the effect of the operating frequency and is given as:

$$A = \left(\frac{4\pi f_c}{c}\right)^{-2}, \tag{10}$$

where c represents the speed of light and f_c represents the operating frequency. Besides, the parameters $\mid \Omega_{sr}[n] \mid$ and $\mid \Omega_{rd_j}[n] \mid$ shown in (8) and (9) are random variables that follow the Rician distribution and are independent and identically distributed (i.i.d). The Rician factor is defined as [12]:

$$K_r\left(\theta_r\left[n\right]\right) = K_{min}\exp\left\{\frac{2}{\pi}\ln\left(\frac{K_{max}}{K_{min}}\right)\theta_r\left[n\right]\right\}, \qquad (11)$$

where K_{min} and K_{max} are the minimum and maximum Rician factor, respectively.

The aerial path loss exponents for the channels between the BS and hybrid RIS-UAV, α_{sr} and between the hybrid RIS-UAV and the UEs, α_{rd_j} are defined as:

$$\alpha_{sr}\left[n\right] = \alpha_e\left(1 - P_{LoS}\left(\theta_{sr}\left[n\right]\right)\right) + \alpha_{o\_sr}, \qquad (12)$$

$$\alpha_{rd_j}\left[n\right] = \alpha_e\left(1 - P_{LoS}\left(\theta_{rd_j}\left[n\right]\right)\right) + \alpha_{o\_rd}, \qquad (13)$$

respectively, where α_e and α_{o_sr}, and α_{o_rd} are constant variables defined by the probability of LoS [12].

Here, Frequency Division Multiple Access (FDMA) is applied to avoid interference between UEs sharing the same time slot. For the hybrid RIS-UAV, the RIS consists of a total of M discrete elements, including L active and $M-L$ passive reflecting elements. Hence, the received signal at each UE is defined as:

$$\begin{aligned} y_j\left[n\right] = {} & \sqrt{P_{bs}}\mathbf{h}_{rd_j}^H\left[n\right]\mathbf{\Phi}\left[n\right]\mathbf{h}_{sr}\left[n\right]s\left[n\right] \\ & + \sqrt{P_{bs}}\mathbf{h}_{rd_j}^H\left[n\right]\mathbf{\Psi}\left[n\right]\mathbf{h}_{sr}\left[n\right]s\left[n\right] \\ & + \mathbf{h}_{rd_j}^H\left[n\right]\mathbf{\Phi}\left[n\right]\mathbf{n}_r\left[n\right] + n_w\left[n\right], \end{aligned} \qquad (14)$$

where P_{bs} represents the transmit power at the BS, s represents the transmitted information signal from the BS, while $\mathbf{n}_r \sim CN\left(0, \sigma_r^2\mathbf{I}_N\right)$ and $n_w \sim CN\left(0, \sigma^2\right)$ represent the thermal noise at the hybrid RIS-UAV and the UEs, respectively. In addition,$\mathbf{\Psi}$and $\mathbf{\Phi}$ represent the reflection matrix of the passive and active elements, respectively, where $\mathbf{\Psi}\left[n\right] = \mathrm{diag}\left\{\mathit{\Psi}_1\left[n\right], \ldots, \mathit{\Psi}_M\left[n\right]\right\}$and $\Phi\left[n\right] = \mathrm{diag}\left\{\mathit{\Phi}_1\left[n\right], \ldots, \mathit{\Phi}_M\left[n\right]\right\}$,

$$\mathit{\Psi}_m\left[n\right] = \begin{cases} 0, & m \in \mathbb{L} \\ e^{j\varphi_m\left[n\right]}, & otherwise \end{cases}, \qquad (15)$$

$$\mathit{\Phi}_m\left[n\right] = \begin{cases} \rho_m\left[n\right]e^{j\varphi_m\left[n\right]}, & m \in \mathbb{L} \\ 0, & otherwise \end{cases}. \qquad (16)$$

The positions of L active elements are denoted as $\mathbb{L} \subset \{1, 2, \cdots, M\}$, and the phase shift of the m-th element is denoted as φ_m, such that $\varphi_m \in [0, 2\pi]$. For simplicity, the amplification gain is identical, i.e., $\rho_m\left[n\right] = \rho\left[n\right]$ for all active elements.

In the scenario of assuming the ideal phase-shifting case, the signal-to-noise ratio (SNR) of both the UEs at n-th time slot is defined as:

$$\gamma_j\left[n\right] = \frac{P_{bs}\left(F_{p_j}\left[n\right] + F_{a_j}\left[n\right]\right)}{\rho\left[n\right]^2\sigma_r^2 L \mid h_{rd_j}\left[n\right] \mid^2 + \sigma^2}, \qquad (17)$$

$$F_{p_j}\left[n\right] = \left(M-L\right)^2 \mid h_{sr}\left[n\right] \mid^2 \mid h_{rd_j}\left[n\right] \mid^2, \qquad (18)$$

$$F_{a_j}\left[n\right] = \rho\left[n\right]^2 L^2 \mid h_{sr}\left[n\right] \mid^2 \mid h_{rd_j}\left[n\right] \mid^2, \qquad (19)$$

while the sum rate of the system is given as:

$$R\left[n\right] = \frac{1}{2}B\log_2\left(1 + \gamma_1\left[n\right]\right) + \frac{1}{2}B\log_2\left(1 + \gamma_2\left[n\right]\right), \qquad (20)$$

where B represents the system bandwidth.

A. Energy Efficiency Maximization Problem

In this paper, the placement of the UAV is optimised to maximise the energy efficiency of the system. The total power consumption of the hybrid RIS-UAV system can be defined as [13]:

$$\begin{aligned} P_{total} = {} & \underbrace{P_{hard\_bs} + P_{hard\_ue} + P_{hard\_uav} + MP_{sw} + LP_{dc}}_{P_{hardware}} \\ & + \underbrace{P_{bs} + P_{ris}}_{P_{comm}}. \end{aligned} \qquad (21)$$

where P_{hard_bs} and P_{hard_ue} are the hardware-dissipated power at the BS and UEs, respectively, P_{hard_uav} represents the power consumption of the UAV while P_{sw} represents the power consumption for controlling the circuit and phase shift switch at each RIS reflecting element, P_{dc} represents the hardware power consumption of active elements, and P_{ris} represents the transmit power at the hybrid RIS-UAV. Therefore, the total power consumption of the system is a combination of hardware power, $P_{hardware}$ and the power for signal transmission, P_{comm}.

The energy efficiency of the hybrid RIS-UAV system is defined as:

$$EE\left[n\right] = \frac{R\left[n\right]}{P_{total}}. \qquad (22)$$

To maximize the energy efficiency, we optimise the placement of the UAV subject to the UAV's permitted altitude range. The optimisation problem is formulated as:

$$\begin{aligned} \max_{\mathbf{w}_{UAV}} \quad & EE\left[n\right], \\ s.t.: \quad & \\ C1: \quad & H_{min} \leqslant z_{UAV}\left[n\right] \leqslant H_{max}, \\ C2: \quad & P_{bs} \parallel \mathbf{\Phi}\mathbf{h}_{sr} \parallel^2 + \sigma_r^2 \parallel \mathbf{\Phi} \parallel^2 \leqslant P_{ris}, \end{aligned} \qquad (23)$$

where the objective function is the energy efficiency of the hybrid RIS-UAV system over a time-varying wireless channel, and the coordinate of the UAV, $\boldsymbol{w}_{UAV}$ is the optimizing parameter. Constraint $C1$ ensures UAV operates within the permitted altitude range, and $C2$ describes the signal amplification ability of the active RIS elements. Since the SNR is monotonically increasing with ρ, hence the optimal ρ^2 can be computed by satisfying the $C2$:

$$\rho^2\left[n\right] = \frac{P_{ris}}{L\left(P_{bs} \mid h_{sr}\left[n\right] \mid^2 + \sigma_r^2\right)}. \qquad (24)$$

Thus, the SNR of the hybrid RIS-UAV with optimised ρ^2 can be computed as:

$$\gamma_j[n] = \frac{P_{bs}\left(P_{bs} \mid h_{sr}[n] \mid^2 + \sigma_r^2\right) F_{p_j}[n]}{P_{ris}\sigma_r^2 \mid h_{rd_j}[n] \mid^2 + \sigma^2\left(P_{bs} \mid h_{sr}[n] \mid^2 + \sigma_r^2\right)} + \frac{P_{bs}P_{ris}L \mid h_{sr}[n] \mid^2 \mid h_{rd_j}[n] \mid^2}{P_{ris}\sigma_r^2 \mid h_{rd_j}[n] \mid^2 + \sigma^2\left(P_{bs} \mid h_{sr}[n] \mid^2 + \sigma_r^2\right)}. \quad (25)$$

B. Optimisation Algorithm

Two optimisation algorithms are studied to optimise the formulated problem, which are Particle Swarm Optimisation (PSO) algorithm and distributed learning algorithm. PSO is a heuristic searching method, first introduced by Kennedy and Eberhart by modeling the social behavior of animals, such as fish schooling and bird flocking [15]. In PSO, we initiate a swarm of particles, each representing a potential UAV position, and the particles cooperate with each other to iteratively update their velocities and positions until obtaining the optimal positions that collectively maximise the energy efficiency of the system. PSO is adopted in this paper because it is simple to implement and it is efficient in balancing the exploitation and exploration [16], as well as the ability to converge towards global optima [17]. The PSO algorithm utilizes MATLAB $particleswarm$ function to find the optimal UAV's coordinate that maximises the energy efficiency of the hybrid RIS-UAV system. The steps are described below:

Step 1: Define the objective function. The objective function is the negative of the energy efficiency function defined as in (22). So, the goal of PSO is to search for the coordinate of the UAV, $\boldsymbol{w}_{UAV}$ that minimise the objective function.

Step 2: Initialisation of the particles within the search space. The number of particles in the swarm is initialised first, and their positions and velocities are randomly assigned within the permitted search space. The position of ith particle in 3 dimension is represented as:

$$X_i = (x_{i1}, x_{i2}, x_{i3}), \quad (26)$$

and the velocity of ith particle is represented as:

$$V_i = (v_{i1}, v_{i2}, v_{i3}). \quad (27)$$

Step 3: Evaluation of the fitness. The fitness of each particle is evaluated by computing the objective function value at its current position.

Step 4: Movement of the particles. By updating the particles' position and velocities based on PSO equation, each particle adjusts its position and velocity according to its own experience, i.e. local minima, and the best position within the swarm, i.e. global optimum. The local minima of ith particle is denoted as:

$$p_{l_i} = (p_{i1}, p_{i2}, p_{i3}), \quad (28)$$

while the global optimum is denoted as:

$$p_g = (p_{g1}, p_{g2}, p_{g3}). \quad (29)$$

Meanwhile, the PSO equations for updating the particles' positions and velocities are as follows:

$$V_i = wV_i + c_1r_1\left(p_{l_i} - X_i\right) + c_2r_2\left(p_g - X_i\right), \quad (30)$$

$$X_i = X_i + V_i, \quad (31)$$

where w is the inertia factor, c_1 and c_2 are the acceleration coefficients, while r_1 and r_2 are the random number between 0 and 1 that introduces stochasticity to the process.

Step 6: Iterative process. The steps 2 to 4 are repeated until the termination condition is met, which is when the maximum number of iterations is reached.

Step 7: Termination and returning of the solution. The solution, which corresponds to the values of the coordinate of the UAV that minimises the objective function, is obtained such that it maximises the energy efficiency function of hybrid RIS-UAV.

To reduce the computational time and complexity of the system, a distributed learning algorithm is proposed, which uses only one particle to search for the optimal position of the UAV that maximises the energy efficiency of the system. The steps for implementing the distributed learning algorithm are as follows:

Step 1: Initialisation of the UAV position. The location of the UAV is first initialised to hover above the BS, with an altitude of H_{max}.

Step 2: Evaluation of the fitness. The distance of the UAV with the UEs is evaluated by moving the UAV in eight different directions (North, Northeast, East, Southeast, South, Southwest, West, and Northwest).

Step 3: Movement of the UAV. The UAV adjust its position with a constant distance to the direction that has the shortest distance from the UEs. If there is more than one shortest distance to the UEs, then the energy efficiency of the specific positions is computed, and the UAV move to the position where it has the highest energy efficiency.

Step 4: Iterative process. Steps 2 to 3 are repeated until moving the UAV produces lower energy efficiency than the previous move. Then, the UAV evaluates the position between the previous position and the current position and moves to the position where it produces the highest energy efficiency.

Step 5: Returning of the optimal position. The solution, which is the optimal position of the UAV is obtained. By using the optimal xy coordinate of the UAV, the UAV evaluates the energy efficiency function by hovering at different permitted heights.

Step 6: Termination and returning of the solution. Once the optimal altitude is determined, the algorithm is terminated as the optimal 3D placement of the UAV that maximises the energy efficiency of the system is obtained.

III. Results and Discussions

In this section, numerical results are presented to evaluate the performance of hybrid RIS-UAV by optimising the placement of the UAV. All the results are obtained through Monte

TABLE I
SIMULATION PARAMETERS

Parameter	Default Value
α_e; α_{o_sr};α_{o_rd}	1.5; 2; 2.4
a; b	11.95; 0.136
K_{min}; K_{max}	5 dB; 15 dB
H_{min}; H_{max}	10; 120
M	256
L	1
f_c	2.3 GHz
B	1 MHz
σ_r^2;σ^2	-90 dBm
P_{sw}	-10 dBm
P_{dc}	-5 dBm
P_{hard_bs}; P_{hard_ue}; P_{hard_uav}	20 dBm
P_{bs}	46 dBm
P_{ris}	20 dBm

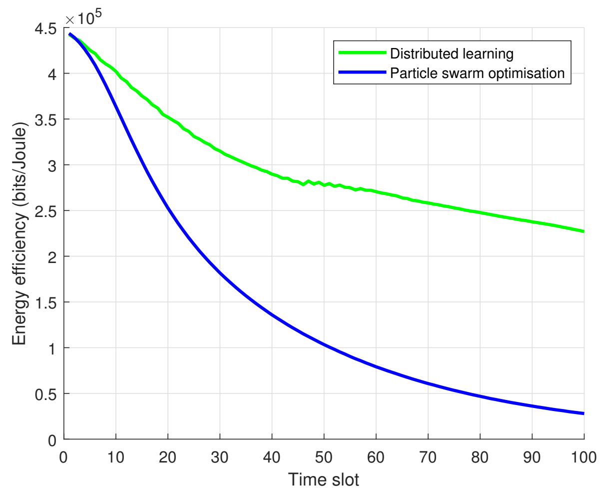

Fig. 2. Energy efficiency performance of different optimisation approaches.

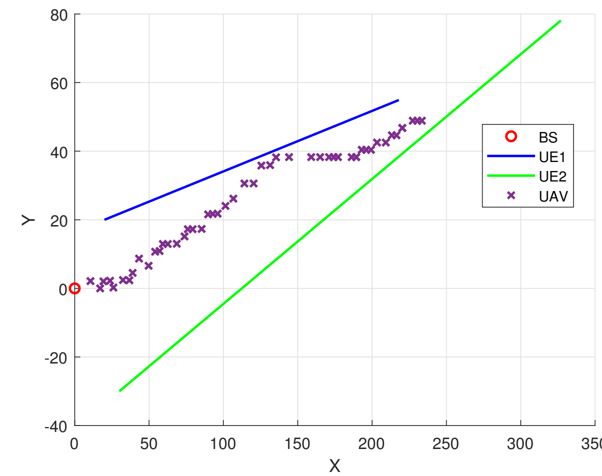

Fig. 3. Location of the nodes.

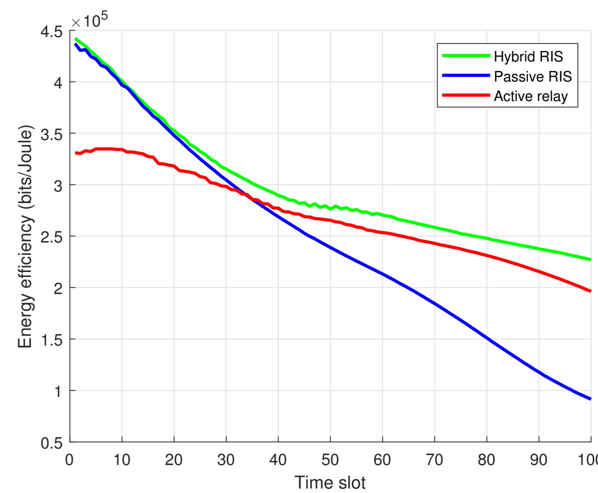

Fig. 4. Energy efficiency performance of different relaying modes.

Carlo simulation with 100,000 samples, and the simulation parameters used are listed in Table 1 [12]–[14]. For the position of the ground nodes, the coordinates of the BS is fixed at $(0, 0, 0)$ while the UE 1 and UE 2 are moving with constant speed in positive x-direction with 10° and 20°, respectively. The initial coordinate of UE 1 is $(20, 20, 0)$ while UE 2 is $(30, -30, 0)$. Whereas, the initial position of the UAV is hovering at coordinate $(0, 0, 120)$. In addition, the environmental parameters are based on dense urban scenarios.

By optimising the placement of the UAV, our proposed distributed learning algorithm produces higher energy efficiency of the system compared to the PSO algorithm, as shown in Fig. 2. This is because the PSO algorithm takes a longer time to compute, hence the UAV continues to hover for the same position throughout the time slot. As the UEs move further, the distance between the UAV and the UEs increases, so the path loss increases, thus degrading the rate and the energy efficiency of the system. On the other hand, our proposed distributed learning algorithm can compute the optimal UAV's coordinate in a shorter time, hence the UAV is able to continue to move to the next optimal position whenever the UEs move. As shown in Fig. 3, when the UEs move in the positive x-direction, the UAV moves in the same direction so as to shorten the distances from the UEs. Since the channel link between the UAV and the UEs is weaker than the channel link between the UAV and the BS, and the signal transmission power is smaller at RIS than BS, hence the rate and energy efficiency are improved when placing the UAV nearer to the UEs. In short, our proposed distributed learning algorithm is better than the PSO algorithm since it reduces the computational time and complexity while producing same performance.

As shown in Fig. 4, the energy efficiency is the highest when hybrid RIS is utilised as the relaying mode compared to the fully passive RIS and active full-duplex amplify-and-forward (AF) relay. This is because the active RIS elements can boost the signal strength with the amplification factor, thus improving the energy efficiency of the system. With a single active element, the hybrid RIS-UAV doubles the energy efficiency of the fully passive RIS-UAV when the distance between BS and UEs increases. As UEs move in each time slot, hence the distances between BS and UEs increases as the time slot increases. When the distance between BS and UEs is small, there is only a small improvement in energy efficiency by comparing hybrid RIS-UAV to the fully passive RIS-UAV, as the double path-loss problem that the fully passive RIS-UAV suffered is minimised, and thus the signal can be received with high SNR. Besides, the energy efficiency of utilising the hybrid RIS-UAV outperforms the active AF relay even though these two relaying technologies amplify the signal in full-duplex mode. This is due to the self-interference that introduces when the transmitted signal interferes with the received signal within the active AF relay itself. On the other hand, hybrid RIS-UAV is free from the self-interference as it reflects the incident signal with amplification gain without receiving it. As a result, hybrid RIS-UAV is preferred when the distance between BS and UEs is large.

Meanwhile, the optimal number of active RIS elements by considering the power consumption is a potential future work to improve the system performance. Besides, the considered system model can be extended to explore the more general case which involves more than two UEs.

IV. Conclusions

The integration of RIS and UAV emerges as a promising solution for the future wireless communication network. Therefore, this paper investigated the energy efficiency maximisation problem of the hybrid RIS-UAV system for the multiple users case, in which the RIS that mounted on the UAV consists of both active and passive elements. To maximise the energy efficiency of the hybrid RIS-UAV system, PSO and distributed learning algorithms are studied to optimise the placement of the UAV. Based on the results simulated, our proposed distributed learning algorithm outperforms the PSO algorithm since it takes a shorter time to compute the optimal solution. As the UEs move, the optimal position of the UAV moves in the same direction as the UEs in order to shorten the distances from the UEs and improve the energy efficiency of the system. By using the proposed distributed learning algorithm, the hybrid RIS-UAV achieves an energy efficiency improvement of twice the fully passive RIS-UAV. In addition, the hybrid RIS-UAV outperforms the conventional active AF relay in terms of energy efficiency. Hence, the application of hybrid RIS-UAV in assisting the ground communication system is promising for improving wireless communication.

Acknowledgment

This work was supported by the Ministry of Higher Education Malaysia under the Fundamental Research Grant Scheme FRGS/1/2020/TK0/UTM/02/68 and Higher Institution Centre of Excellence (HICOE) Grant 09465, and by Universiti Teknologi Malaysia under Grant 22H33, in part by H2020-MSCA-RISE-2020 under Grant 101008085, and in part by the China Guangxi Science and Technology Plan Project (Guangxi Science and Technology Base and Talent Special Project) under Grant AD23026096 (Application Number 2022AC20001), Chile CONICYT FONDECYT Regular under Grant 1181809, and Chile CONICYT FONDEF under Grant ID16I10466. The authors would also like to acknowledge the support of the 5GIC/6GIC members for this work.

References

[1] Q. Wu, S. Zhang, B. Zheng, C. You, and R. Zhang, “Intelligent reflecting surface-aided wireless communications: A tutorial,” IEEE Transactions on Communications, vol. 69, pp. 3313–3351, 2021.

[2] A. C. Pogaku, D.-T. Do, B. M. Lee, and N. D. Nguyen, “UAV-assisted RIS for future wireless communications: A survey on optimization and performance analysis,” IEEE Access, vol. 10, pp. 16 320–16 336, 2022.

[3] K.-W. Park, H. M. Kim, and O.-S. Shin, “A survey on intelligent-reflecting-surface-assisted UAV communications,” Energies, vol. 15, no. 14, p. 5143, Jul 2022.

[4] M. Munochiveyi, A. C. Pogaku, D. Do, A. Le, M. Voznák, and N. D. Nguyen, “Reconfigurable intelligent surface aided multi-user communications: State-of-the-art techniques and open issues,” IEEE Access, vol. 9, pp. 118 584– 118 605, 2021.

[5] C.Y. Goh, C.Y. Leow, and R. Nordin, “Energy efficiency of unmanned aerial vehicle with reconfigurable intelligent surfaces: a comparative study,” Drones, vol. 7, no. 2, pp. 98, 2023.

[6] X. Pang, M. Sheng, N. Zhao, J. Tang, D. Niyato, and K. Wong, “When UAV meets IRS: expanding air-ground networks via passive reflection,” IEEE Wireless Communications, vol. 28, no. 5, pp. 164–170, 2021.

[7] D. Wang, Y. Zhao, Y. He, X. Tang, L. Li, R. Zhang, and D. Zhai, “Passive beamforming and trajectory optimization for reconfigurable intelligent surface-assisted UAV secure communication,” Remote Sensing, vol. 13, no. 21, p. 4286, 2021.

[8] T. Shafique, H. Tabassum, and E. Hossain, “Optimization of wireless relaying with flexible UAV-borne reflecting surfaces,” IEEE Transactions on Communications, vol. 69, no. 1, pp. 309–325, 2021.

[9] N. T. Nguyen, Q.-D. Vu, K. Lee, and M. Juntti, “Hybrid relay-reflecting intelligent surface-assisted wireless communications,” IEEE Transactions on Vehicular Technology, vol. 71, pp. 6228–6244, 2022.

[10] A. Al-Hourani, S. Kandeepan, and S. Lardner, “Optimal lap altitude for maximum coverage,” IEEE Wireless Communications Letters, vol. 3, pp. 569– 572, 2014.

[11] M. M. Azari, F. Rosas, K.-C. Chen, and S. Pollin, “Ultra reliable UAV communication using altitude and cooperation diversity,” IEEE Transactions on Communications, vol. 66, pp. 330–344, 2018.

[12] W. K. New, C. Y. Leow, K. Navaie, and Z. Ding, “Robust non-orthogonal multiple access for aerial and ground users,” IEEE Transactions on Wireless Communications, vol. 19, pp. 4793–4805, 2020.

[13] K. Zhi, C. Pan, H. Ren, K. K. Chai, and M. Elkashlan, “Active RIS versus passive RIS: which is superior with the same power budget?” IEEE Communications Letters, vol. 26, no. 5, pp. 1150–1154, 2022.

[14] M. F. Sohail, C. Y. Leow and S. Won, “Energy-efficient non-orthogonal multiple access for UAV communication system,” in IEEE Transactions on Vehicular Technology, vol. 68, no. 11, pp. 10834-10845, Nov. 2019.

[15] J. Kennedy and R. Eberhart, “Particle swarm optimization,” in Proceedings of ICNN’95 - International Conference on Neural Networks vol. 4, pp. 1942-1948, 1995.

[16] T. M. Shami, A. El-Saleh, M. Alswaitti, Q. Al-Tashi, A. Summakieh, and S. Mirjalili, “Particle swarm optimization: A comprehensive survey,” IEEE Access, pp. 1–1, 2022.

[17] W. Zhang and W. Zhang, “An efficient UAV localization technique based on particle swarm optimization,” IEEE Transactions on Vehicular Technology, vol. 71, no. 9, pp. 9544–9557, 2022.